Supplementary figure 1

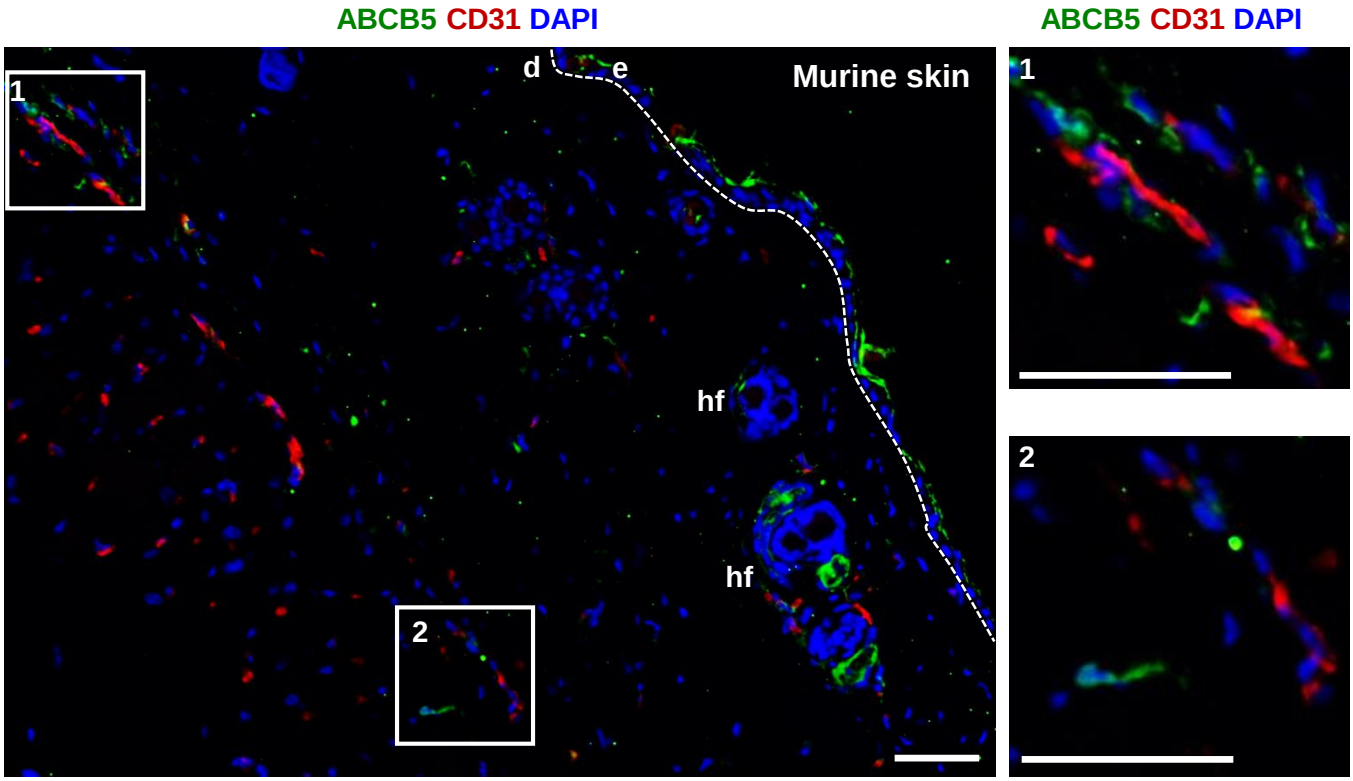

Supplementary figure 1. Localization of ABCB5$^+$ MSCs in healthy murine skin
Microphotographs of 5µm sections from murine skin subjected to immunostaining for ABCB5 (green) and the endothelial marker CD31 (red) revealed both a perivascular (1) and a dispersed interfollicular dermal localization (2) of ABCB5$^+$ cells. The hair follicles are transversally cut, and the unspecific staining (autofluorescence) of the roundish structure represents a hair which is dislocated by cutting the biopsy. Nuclei of all studied skin sections were counterstained with DAPI (blue). Scale bars: 50µm; e = epidermis; d = dermis; hf, hair follicle, transversally cut. Dashed white line delineates epidermal from dermal layers.

Supplementary figure 2

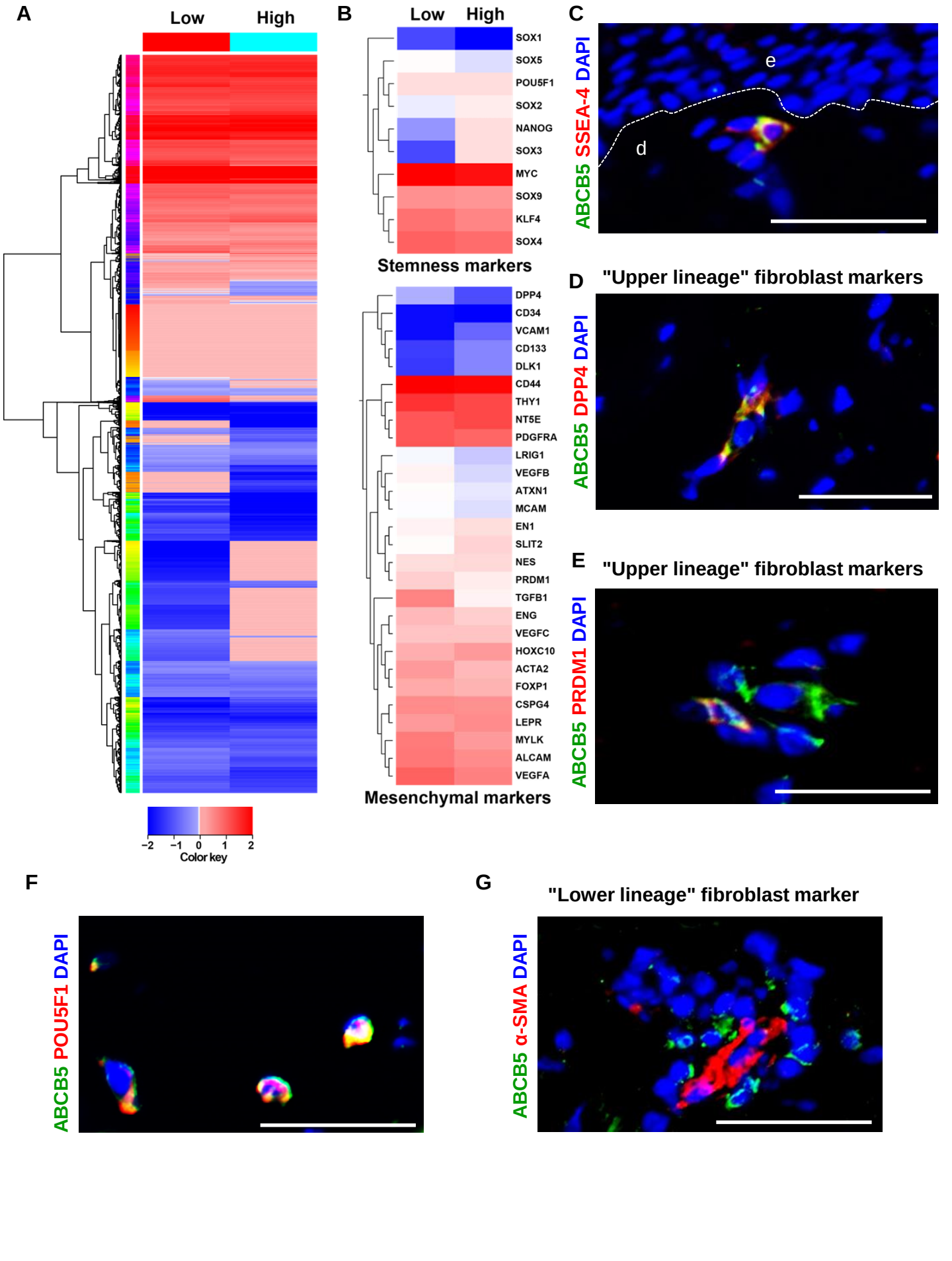

Supplementary figure 2. ABCB5^{+} MSCs may belong to upper rather than lower fibroblast lineage

(A) Heatmap depicting transcriptome profiling of samples (n=3) from low (2-3) and high (above 10) passaged ABCB5^{+}-derived MSCs. The color reflects the log2 scale of relative expression. **(B)** Heatmap depicting genes involved in the maintenance of stemness from early and late passaged ABCB5^{+}-derived MSCs. **(C)** A clear co-localization of ABCB5 (green) with the stem cell marker SSEA-4 (red) was observed in a distinct subpopulation of dermal cells (yellow overlay). **(D-E)** Microphotographs of human skin subjected to double immunofluorescence staining for ABCB5 (green) and the two marker proteins of "upper lineage" fibroblasts (red) revealed a co-expression of ABCB5 with DPP4 (CD26) and a partial co-localization of ABCB5 and PRDM1 (BLIMP1). **(F)** A co-localization of ABCB5 (green) with the stem cell marker POU5F1 (OCT-4) (red). **(G)** ABCB5 (green) was consistently not found co-expressed with the lower lineage fibroblast and myofibroblasts marker α-smooth muscle actin (α-SMA) (red). Nuclei of all studied skin sections were counterstained with DAPI (blue). Scale bars: 50μm; e = epidermis; d = dermis. Dashed white line delineates epidermal from dermal layers.

Supplementary figure 3

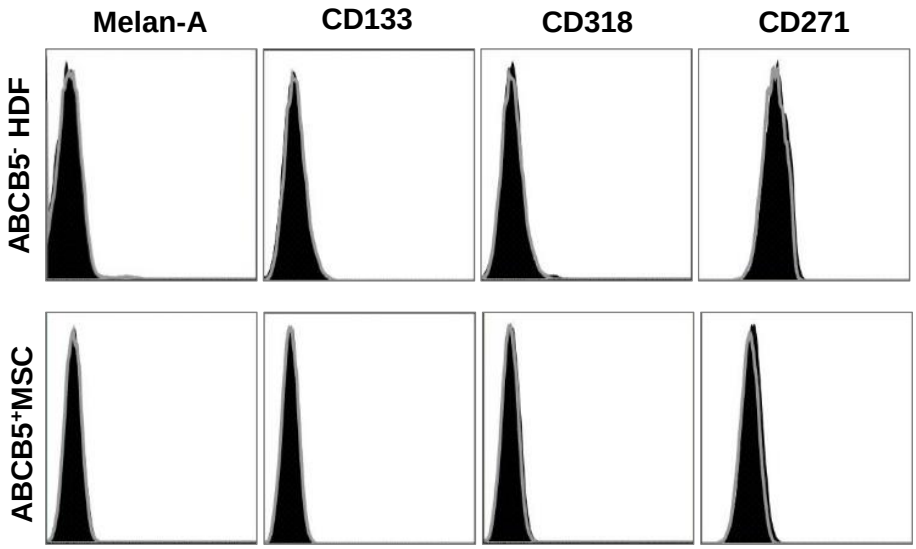

Supplementary figure 3. ABCB5^{+} sorted dermal MSC marker expression profile
Both ABCB5^{+} and ABCB5^{-} sorted plastic-adherent human dermal cells were negative for Melan-A, CD133, CD318 and CD271 by flow cytometry (black histograms) as shown here in overlay with the respective isotype controls (grey lines). All histograms show data obtained for donor B03 (Table S1) and are representative for dermal cell fractions from six donors.

Supplementary figure 4

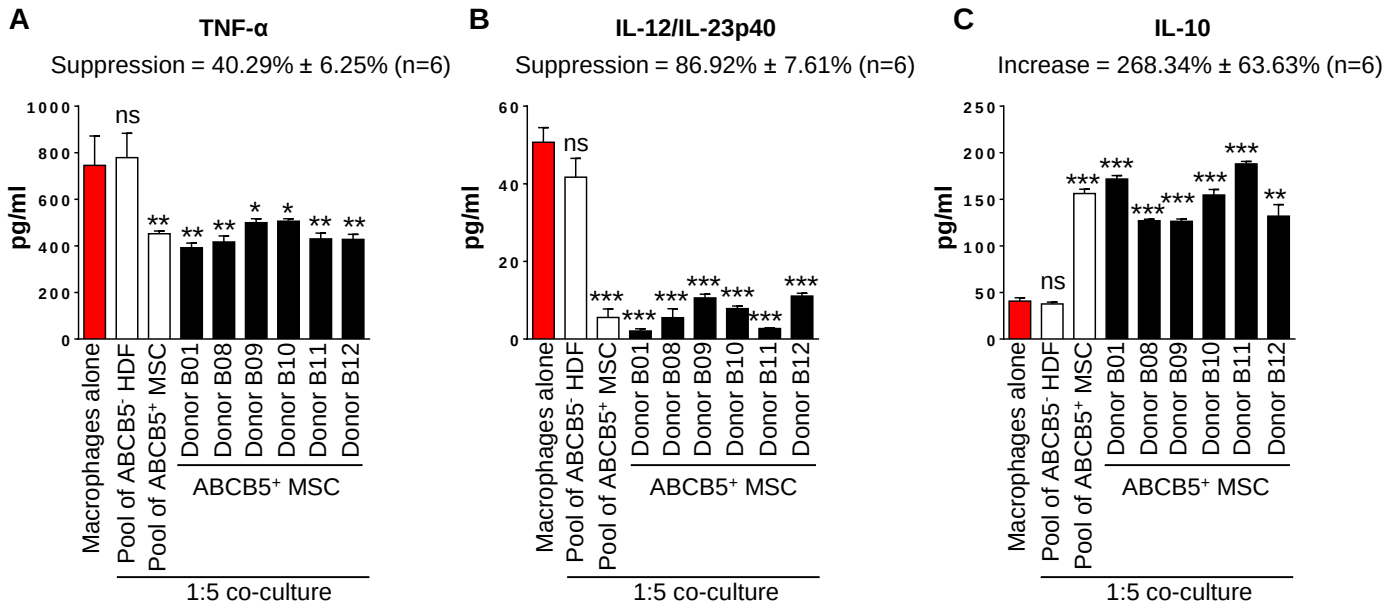

Supplementary figure 4. Modulation of activated macrophages by ABCB5⁺ MSCs from multiple donors

(A-C) The *in vitro* anti-inflammatory effect on classically (by IFN-γ + LPS) activated macrophages at an MSC : macrophage ratio of 1:5 is shown for both the pooled samples as well as for the ABCB5⁺ sorted dermal MSCs from the individual donors (B01, B08, B09, B10, B11 and B12; Table S1) that comprise the pooled donors sample. Co-culture of human dermal ABCB5⁺ -derived MSC with human macrophages matured from peripheral blood monocytes at a ratio of 1:5 significantly downregulates the secretion of the pro-inflammatory M1 cytokines TNFα (left) and IL-12/IL-23p40 (middle) upon classical IFN-γ/LPS activation while upregulated The anti-inflammatory M2 cytokine IL-10 (right) as measured by ELISA. ns = not significant; * $p < 0.05$; ** $p < 0.01$; *** $p < 0.001$, t-test.

Supplementary figure 5

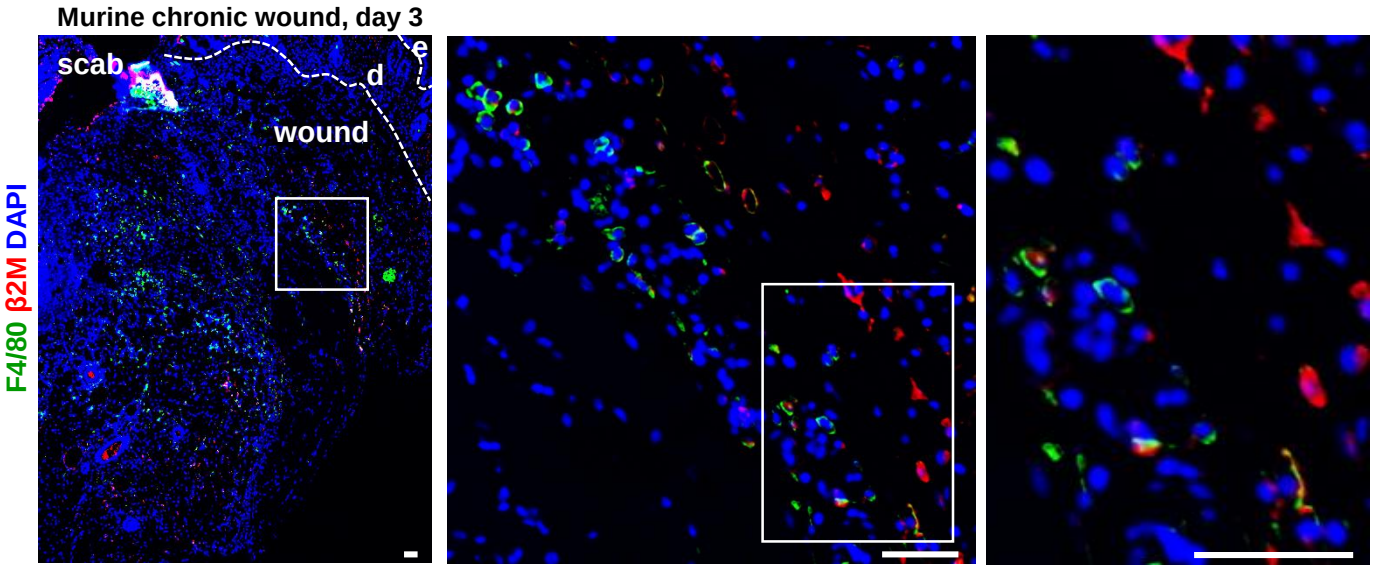

Supplementary figure 5. In the wound bed, injected ABCB5⁺ MSCs are localized close to endogenous macrophages

Double immunofluorescence staining of endogenous murine macrophages (F4/80, green) in day 3 iron overloaded chronic wound beds with human specific β2 microglobulin (red) shows the injected human ABCB5⁺ MSCs close to endogenous macrophages. An overview (left panel) with higher magnification of the indicated rectangle (middle and right panel). Nuclei were counterstained with DAPI (blue). Scale bars: 50µm; e = epidermis; d = dermis.

Supplementary figure 6

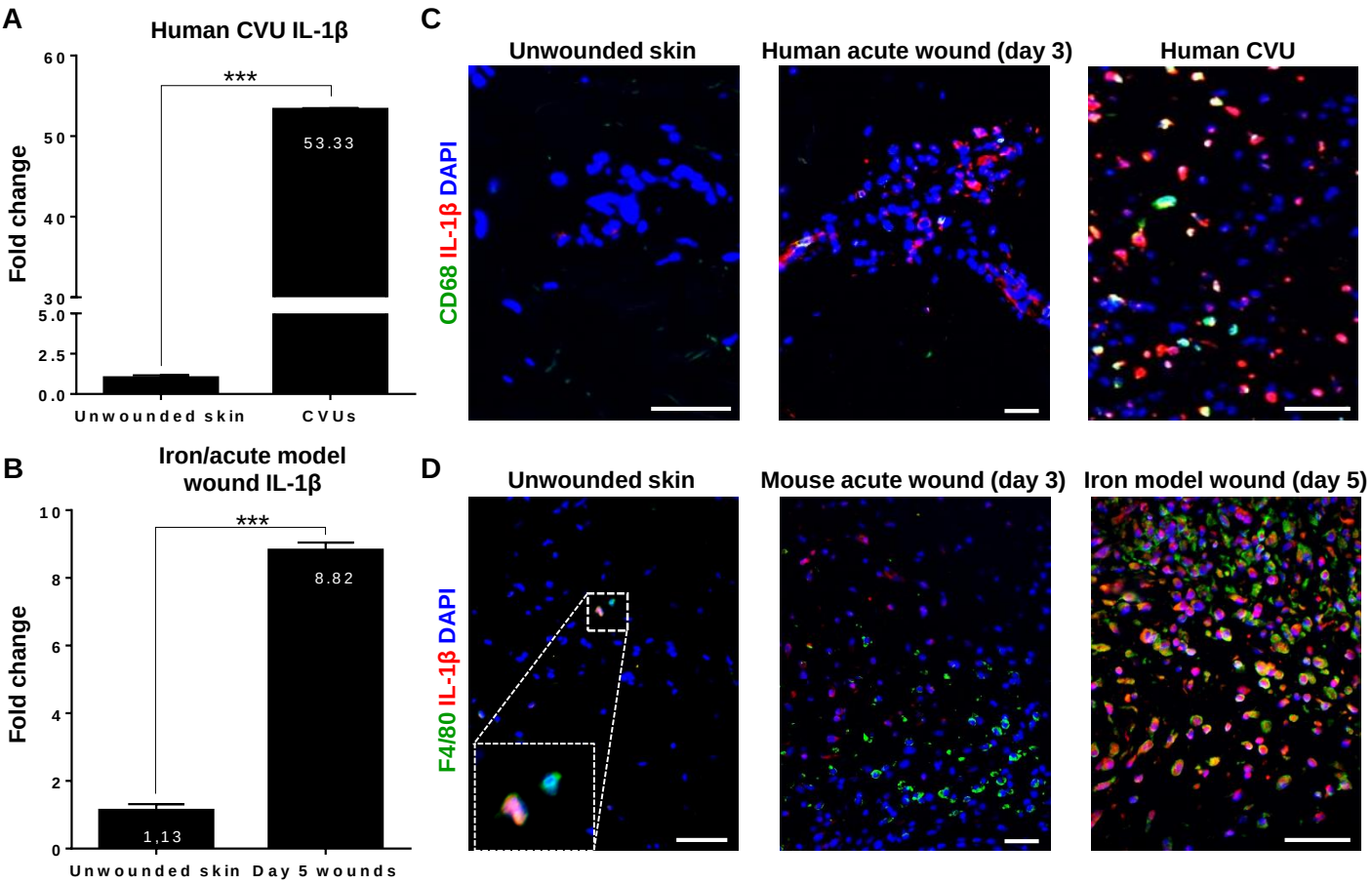

Supplementary figure 6. IL-1β expression is highly increased in human CVU and wounds of iron overload mice

(**A**) Specific mRNA levels for IL-1β were highly increased in human chronic venous leg ulcers (CVU) compared to human healthy skin as assessed by qPCR. (**B**) The ratio of IL-1β mRNA expression in wounds of iron overload mice to wounds of acute wound healing model mice is highly increased compared to the ratio of IL-1β expression in healthy skin of both model systems. (**C**) Representative microphotographs of human skin sections confirm high IL-1β expression in human CVU compared to normal skin of donor A14 (Table S1) and to an acute wound. (**D**) Co-immunostaining for the murine macrophage marker F4/80 (green) and IL-1β (red) of murine iron-model skin and murine iron model wound sections show macrophages as a main source of IL-1β in iron model wounds and confirm a higher IL-1β expression in iron model wounds compared to healthy skin as well as to murine acute wounds. (A, B) n=3; (C) scale bars = 100µm; e = epidermis; d = dermis. Dashed line delineates epidermis from dermis. (D) Scale bars = 50µm. Nuclei were stained with DAPI (blue). *** $p < 0.001$, t-test.

Supplementary figure 7

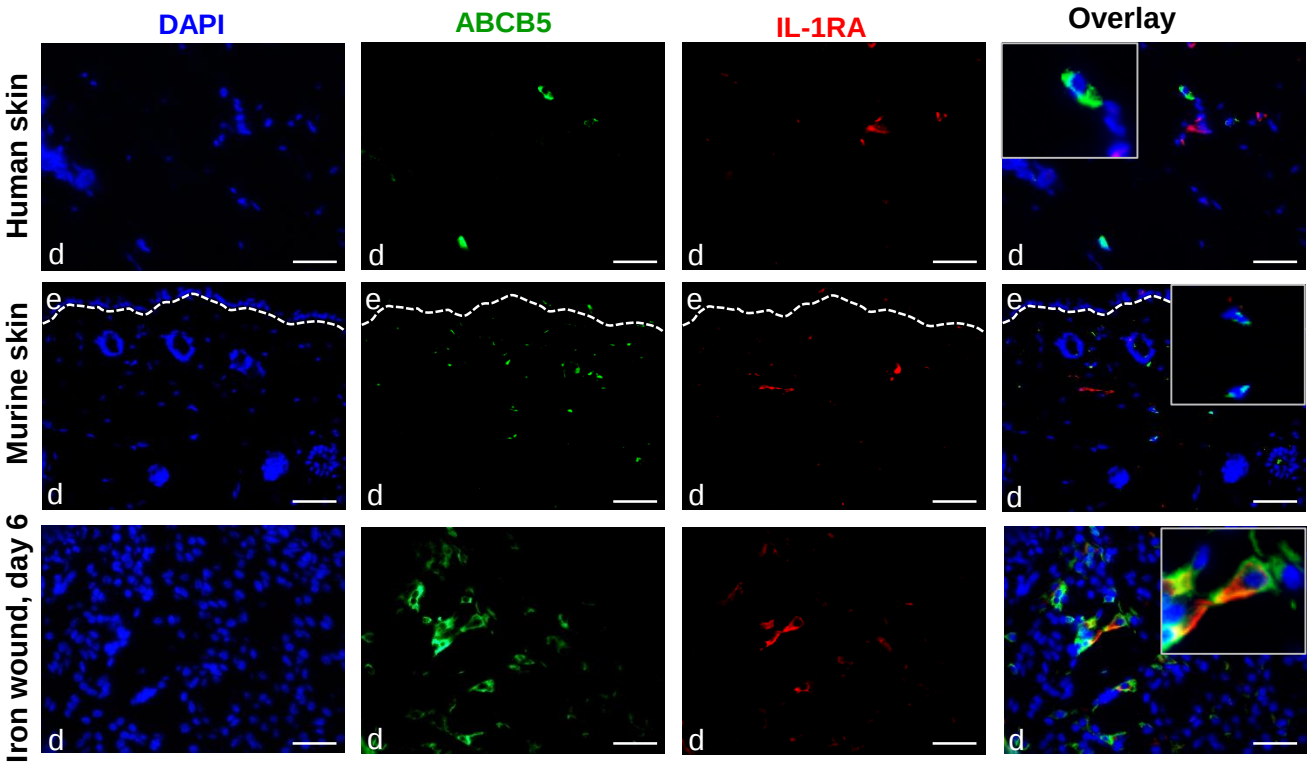

Supplementary figure 7. Endogenous murine ABCB5$^+$ MSCs express IL-1RA in iron overload wounds

Representative microphotographs of co-immunostainings for ABCB5 (green) and IL-1RA (red) show ABCB5$^+$ cells in their endogenous niches in human healthy skin, murine healthy skin and iron overload model mouse wounds treated with PBS injection at day 6. In unwounded healthy skin, neither human nor murine endogenous ABCB5$^+$ MSCs co-expressed IL-1RA. By contrast, a strong co-expression of ABCB5 and IL-1RA was observed in chronic wounds of the iron-overload model. Moreover, the number of ABCB5 positive cells was found to be increased. Scale bars = 50µm.

Supplementary figure 8

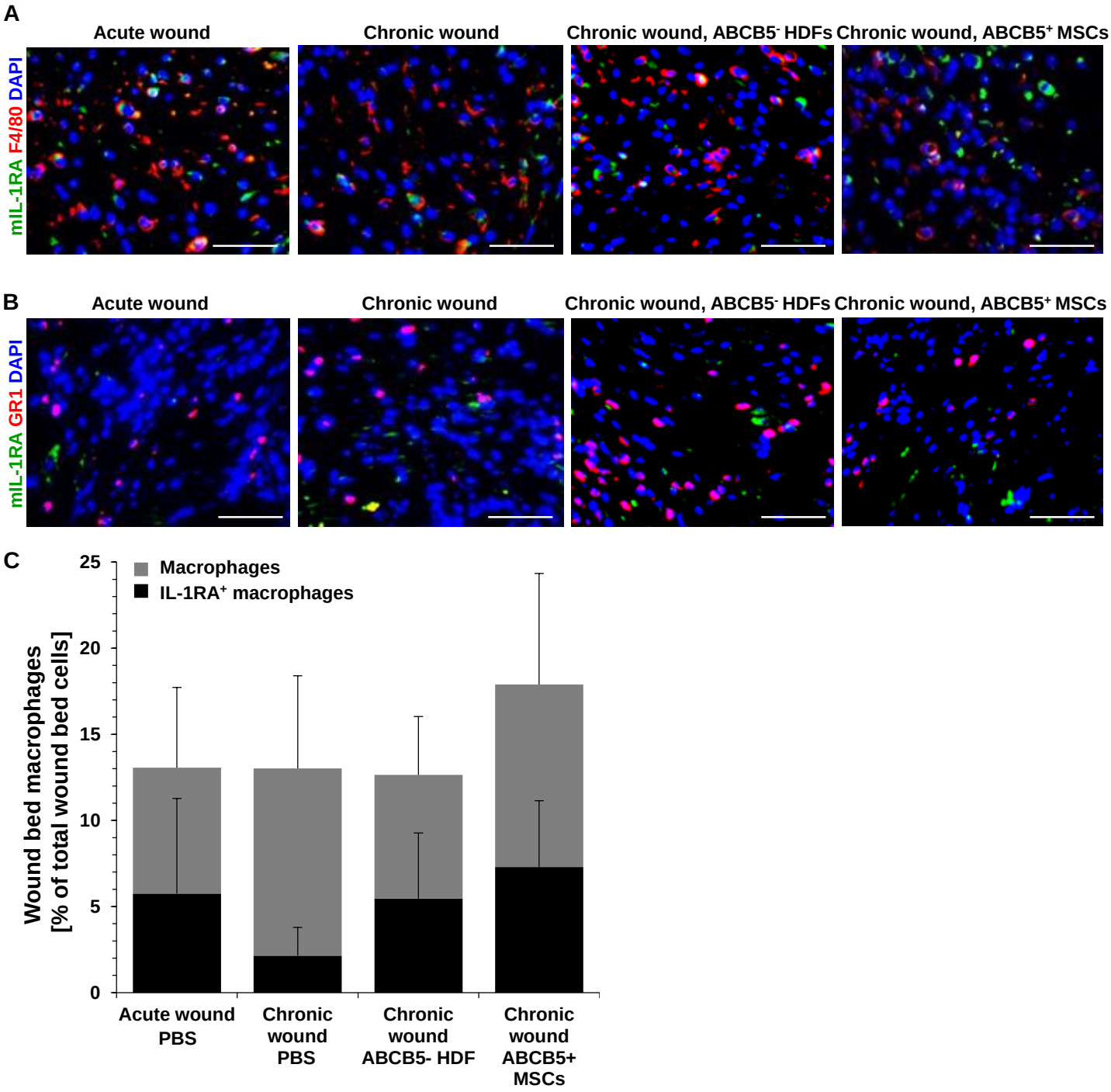

Supplementary figure 8. Endogenous IL-1RA production by macrophages is independent of MSC treatment

Double immunofluorescence staining of endogenous murine IL-1RA (green) in day 3 acute (first panel) and iron overloaded chronic wound beds (three right panels) with markers for (**A**) macrophages (F4/80, red) and (**B**) neutrophil granulocytes (GR1, red) shows that endogenous IL-1RA is produced by a subpopulation of murine macrophages but not by neutrophils. (**C**) Treatment of chronic mouse wounds with either ABCB5$^-$ cell or ABCB5$^+$ MSC injection did not change the proportion of macrophages producing IL-1RA. Nuclei of all studied wound sections were counterstained with DAPI (blue). Scale bars: 50µm.

Supplementary figure 9

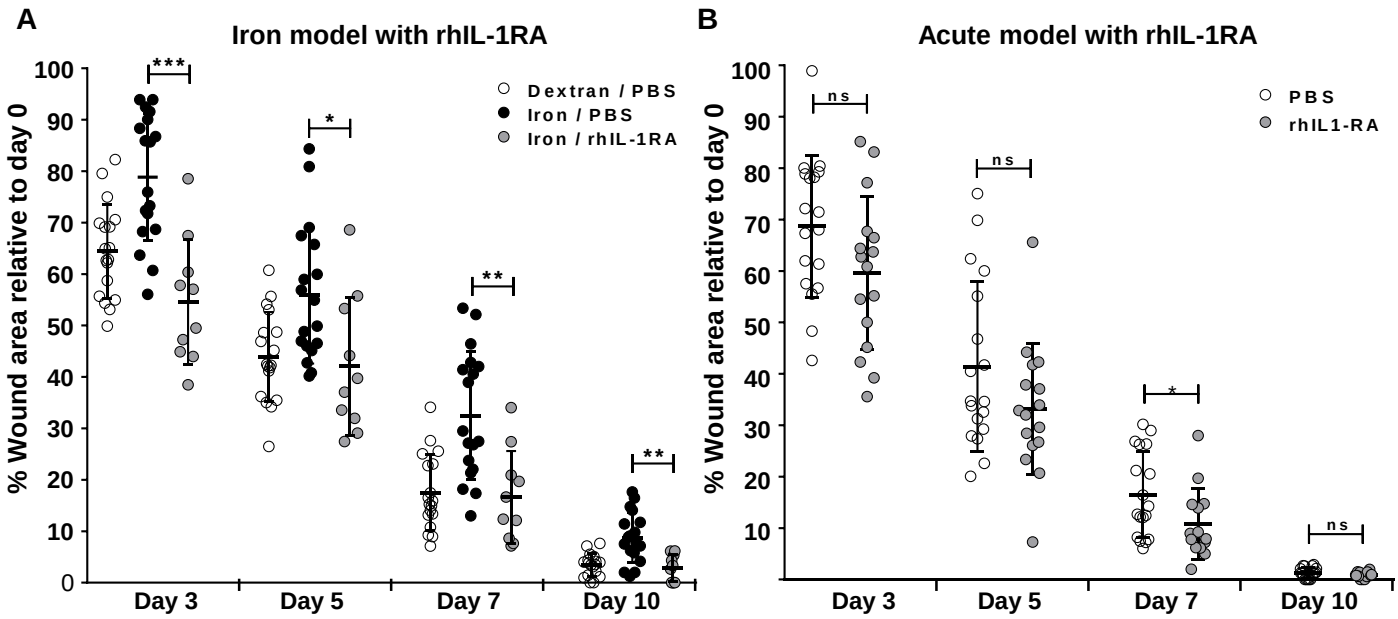

Supplementary figure 9. Recombinant human IL-1RA treatment of iron model and acute model wounds. (**A**) Intradermal injection of 250ng/wound rhIL-1RA in PBS around the wound edge at day one post-wounding (grey), significantly accelerated wound closure of iron-overload mice as compared to injection with PBS alone (black) to a rate comparable with acute model full-thickness excisional mouse wounds (open). (**B**) By contrast, rhIL-1RA injection in to acute wounds (grey) was unable to significantly accelerate wound closure (except for a minor effect at day 7), when compared to PBS injected wound (open symbols). ns = not significant; * $p < 0.05$; ** $p < 0.01$; *** $p < 0.001$, t-test.

Supplementary figure 10

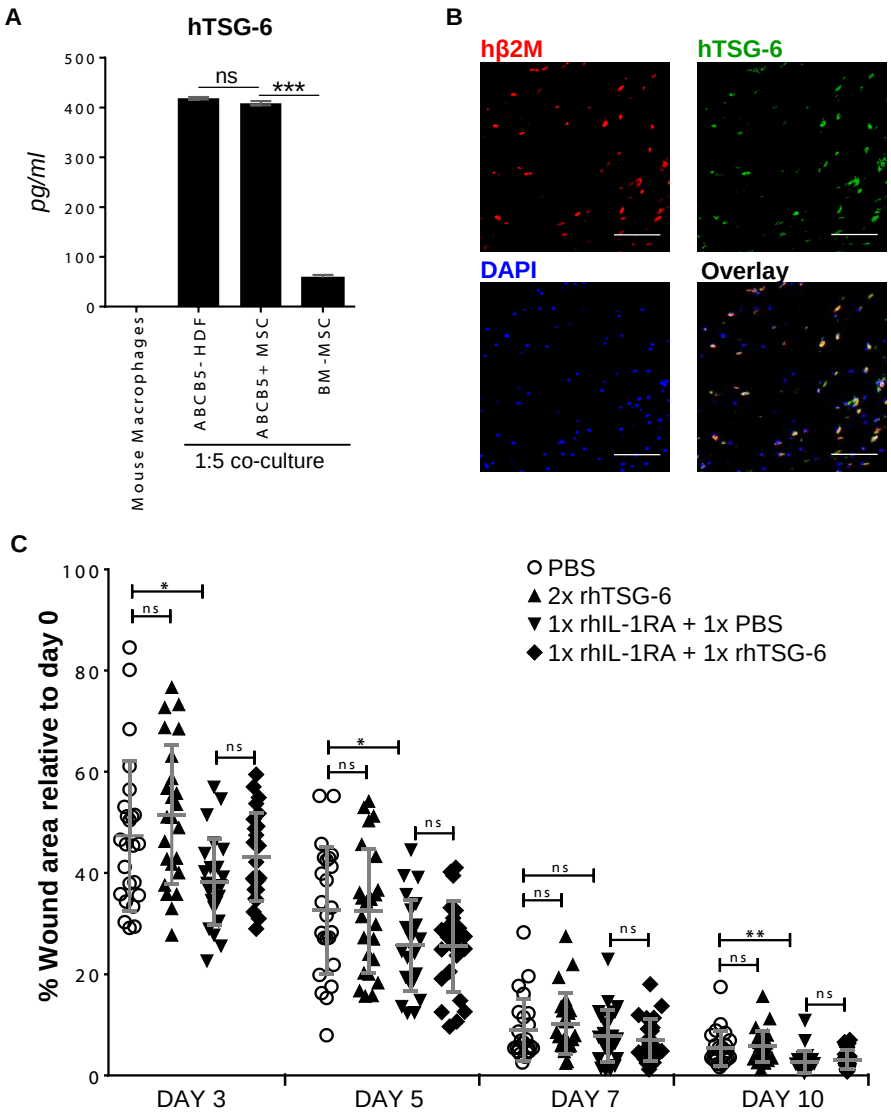

Supplementary figure 10. rhTSG-6 administration does not accelerate wound healing in iron model.

(A) Both ABCB5^{+} MSCs and ABCB5^{-} HDFs produced TSG-6 to a higher extent than BM-MSCs upon co-culture with classically activated mouse macrophages. **(B)** Similarly to IL-1RA, also TSG-6 production by ABCB5^{+} MSCs was evident by double immunostaining with antibodies directed against β2M and TSG-6 *in vivo* 6h after intradermal injection around iron model wound edges. Scale bars = 50μm, staining with DAPI for the nuclei (blue). **(C)** Wound closure in iron overloaded mice (○) was accelerated with rhIL-1RA (▼), but not with rhTSG-6 (▲) injections at a time-dose regiment that significantly accelerated wound closure in acute full-thickness excisional wounds of mice. A presumed synergistic effect between rhIL-1RA and rhTSG-6 (♦) was not observed. Wound size analysis was performed blinded for this experiment. ns = not significant; * $p < 0.05$; ** $p < 0.01$; *** $p < 0.001$, t-test.

Supplementary figure 11

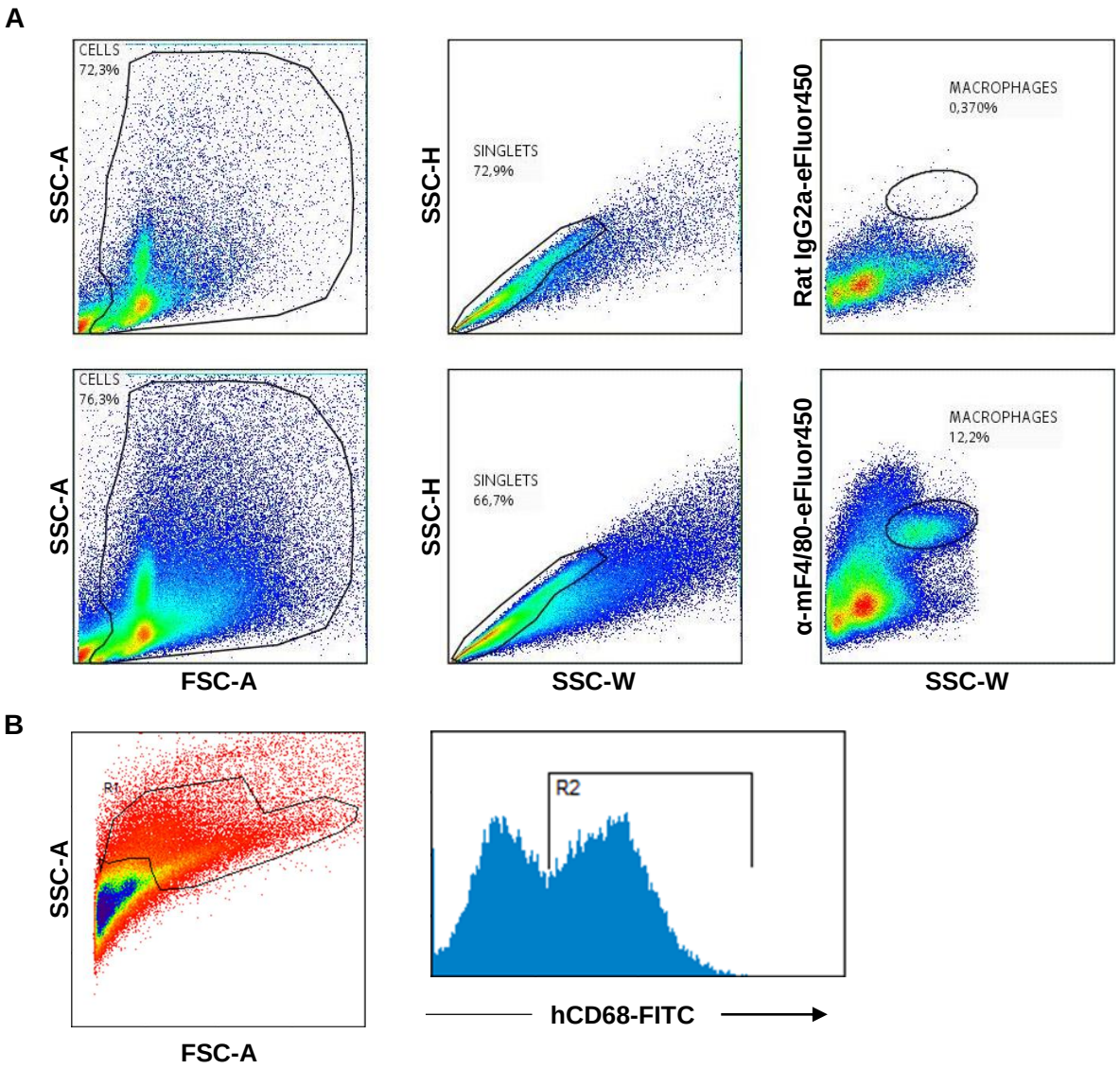

Supplementary figure 11. Flow cytometry analysis for mouse and human wound macrophage immune-phenotyping

(**A**) Singlet cells by scatter characteristics (left and middle) were further gated by F4/80-eFluor450 expressing events for further M1/M2-marker analysis (right). This gating strategy allowed for the identification of a substantial F4/80^{+} mouse macrophage population (bottom) compared to the respective eFluor450-conjugated isotope control staining (top). (**B**) Debris was excluded by gating for scatter characteristics. Gating of human macrophages was performed in the anti-human specific CD68-FITC channel.

Supplementary Materials and Methods

Expansion and isolation of ABCB5$^+$ and ABCB5$^-$ dermal cell fractions

Plastic adherent dermal cells were expanded at the maximum for 16 passages equaling a cumulative population doubling of 25 and separated into ABCB5$^+$ and ABCB5$^-$ fractions by respective two and three consecutive rounds of magnetic bead sorting with mouse anti-human ABCB5 IgG_1 antibody (clone UG3C2-2D12;(*47*)). More than 90% sort purity is one of the release criteria of GMP-grade dermal ABCB5$^+$ cells (Table S2). By flow cytometry, average purity of ABCB5$^+$ cells was 98.33% ± 1.12% (n = 243). For experiments, sorted cells were either cryopreserved or cultured up to a maximum of 72 hours. Purity at this time-point was typically > 70%. ABCB5$^+$ dermal MSCs were cultured in Ham´s F10 supplemented with 15% heat-inactivated high quality fetal bovine serum, 6mM HEPES, 2.8µg/ml hydrocortisone, 100U/ml penicillin/streptomycin, 2mM L-glutamine, 10µg/ml insulin, 0.2mg/ml glucose, 6.16ng/ml PMA (Sigma-Aldrich) and 0.6ng/ml recombinant human basic fibroblast growth factor (Prospecbio), at 37°C and 3% CO_2. Versene (Gibco) was used to detach ABCB5$^+$ dermal cells from the culture plastic. ABCB5$^-$ HDFs were maintained in DMEM with 10% high quality fetal bovine serum, 100U/ml penicillin/streptomycin and 2mM L-glutamine (Biochrom), at 37°C and 5% CO_2.

The C57BL/6 mouse model relevant for CVU pathophysiology

C57/BL/6 mice were injected intraperitoneally seven times with 5mg/200µl iron-dextran or 200µl PBS-Dextran (Sigma-Aldrich) on a three day interval. One day after the last iron injection, four 6mm full-excisional wounds were inflicted with biopsy punchers (Stiefel) on the dorsal skin of shaved mice while under anesthesia. Wounds were photographed next

to a lineal measure in order to quantify the wound areas using Adobe Photoshop software (Adobe Systems).

IL-1β Quantitative PCR

Total RNA was isolated from human chronic venous leg ulcers (CVUs), murine wounds and corresponding healthy control skin using a commercial kit (RNeasy Microarray Tissue Mini Kit, Qiagen) as described by the manufacturer. Two µg of RNA per sample were reverse transcribed using illustra Ready-To-Go RT-PCR Beads (GE Healthcare). Quantity and quality of total RNA and cDNA were assessed using Nanodrop 1000 (Thermo Scientific) and QIAxcel Advance system (Qiagen). The 7300 real time PCR system (Applied Biosystems, Life Technologies) was used to amplify cDNA using Power SYBR green master mix (Applied Biosystems, Life Technologies). Primers specific for human IL-1β (FW: 5'-CCCAAGCAATACCCAAAGA-3' and REV: 5'-CCACTTTGCTCTTGACTTCTA-3') and mouse IL-1β (FW: 5'-TCACAAGCAGAGCACAAG-3' and REV: 5'-GAAACAGTCCAGCCCATAC-3') were used for data given in Fig. S6.

Supplementary table 1. Human skin donors

(**A**) Donor data of healthy skin used in this study for *in vivo* characterization of ABCB5$^+$ dermal cells and of CVU for IL-1β immunostaining of CVU and normal human skin (Fig. S1 and S6). (**B**) Donor data of healthy skin used in this study for dermal cell ABCB5-sorting. *A pool of cells from donors B01, B08, B09, B10, B11 and B12 was used for Figures 3-7 after testing for anti-inflammatory capacity of ABCB5$^+$ dermal MSCs of each donor and the pooled sample (Fig. S4).

A: Donor data of healthy skin used in this study for *in vivo* characterization of ABCB5$^+$ dermal cells and of CVU for IL-1β immunostaining of CVU and normal human skin

Donor ID	Gender (m/f)	Age at biopsy (*yrs*)	Skin biopsy location	Figure Nr(s).
A01	m	19	Lower leg	1B
A02	f	15	Upper belly	1B
A03	f	20	Shoulder	1B
A04	f	18	Lower leg	1B
A05	m	13	High-parietal	1B
A06	f	38	Shoulder	1B
A07	f	42	Lumbal region	1B
A08	m	33	Lower back	1B
A09	m	26	Back	1B
A10	m	38	Neck	1A-B
A11	f	74	Shoulder	1A
A12	f	16	Gluteal region	1C-F
A13	f	62	Breast	1C-F, S7
A14	m	73	CVU + normal control (parallel lower extremities)	S6

B: Donor data of healthy skin used in this study for dermal cell ABCB5-sorting

Donor ID	Gender (m/f)	Age at biopsy (*yrs*)	Skin biopsy location	Figure Nr(s).
B01	f	58	Behind left ear	2A, 3D, 4B-E, 5, 7, S3
B02	f	19	Gluteal region	2D-H (graphs)
B03	m	20	Gluteal region	2 (graphs + pictures), S4
B04	f	20	Gluteal region	2D-H (graphs)
B05	f	20	Gluteal region	2D-H (graphs)
B06	f	19	Inside upper arm	2D-H (graphs)
B07	m	27	Upper arm	2D-H (graphs)
B08	f	66	Behind left ear	S3
B09	f	51	Behind left ear	S3
B10	m	76	Behind left ear	S3
B11	m	51	Behind left ear	S3
B12	f	76	Behind left ear	S3
B13	m	51	Behind left ear	not shown
B14	m	75	Behind left ear	not shown
B01+B08+B09+B10+B11+B12*	-	-	Behind left ear	3-7, S3

**Pooled-donor cell samples*

Supplementary table 2. Release criteria for GMP-compliant dermal ABCB5^{+} MSC preparations used in this study

Parameter	Test Method	Specification
Total count viable cells	Flow cytometry	≥ 90%
Cell vitality	Flow cytometry	≥ 90%
Microbiological control cellular products	Adapted	No growth
Mycoplasma	NAT	Not detectable, <10CFU/ml
Endotoxin level	LAL-test	≤ 2 EU/ml
Cell viability	Flow cytometry	≥ 75%
CD90 surface expression	Flow cytometry	≥ 90%
Bead residues	Flow cytometry	≤ 0.5 %
Content of ABCB5-positive cells	Flow cytometry	≥ 90%
Potency Assay (angiogenic)	Immunofluorescence	Tube formation assay

Supplementary table 3. List of antibodies used in this study

A: Primary antibodies used for immunostaining

Epitope	Clone	Species	Applied reactivity	Company/Reference
ABCB5 (RFGAYLIQAGRMTPEG)	3C2-1D12	Mouse IgG1	Human, mouse	(*47*)
Aggrecan	Polyclonal	Goat IgG	Human	R&D Systems #AF1220
CD31	Polyclonal	Rabbit IgG	Human, mouse	Abcam #28364
CD68	Y1/82A	Mouse IgG2b κ	Human	BD #556059
CD206	Polyclonal	Rabbit	Human	Abcam #64693
F4/80	BM8	Rat IgG2a κ	Mouse	eBioscience #14-4801-85
β2 microglobulin	Polyclonal	Rabbit	Human	Abcam #87483
IL-1β	Polyclonal	Rabbit	Human	Sdix #2360.00.02
IL-1β	Polyclonal	Rabbit	Human, mouse	Abcam #9722
IL-1RA	EPR6483	Rabbit IgG	Mouse	Abcam #124962
NG2	Polyclonal	Rabbit IgG	Human	Millipore #AB5320
SOX2	D6D9	Rabbit IgG	Human	Cell Signaling #3579
SSEA4	Polyclonal	Rabbit IgG	Human	Bioss #bs-3609R
TSG-6	A38.1.20	Rat IgG	Human	Santa Cruz sc-65886
TNFα	Polyclonal	Rabbit	Human	Abcam #183896

B: Flow cytometry antibodies

Epitope	Clone	Species	Applied reactivity	Company/Reference
ABCB5 (RFGAYLIQAGRMTPEG)	3C2-1D12	Mouse IgG1	Human	(*47*)
CD14-PerCp	TÜK4	Mouse IgG2a	Human	Miltenyi Biotec #130-095-198
CD20-PerCp	LT20.B4	Mouse IgG1	Human	Miltenyi Biotec #130-095-198
CD34-PerCp	AC136	Mouse IgG2a	Human	Miltenyi Biotec #130-095-198
CD45-PerCp	5B1	Mouse IgG2a	Human	Miltenyi Biotec #130-095-198
CD68-FITC	eBioY1/82A	Mouse IgG2b κ	Human	eBioscience #11-0689-42
CD73-APC	AD2	Mouse IgG1	Human	Miltenyi Biotec #130-095-198
CD90-FITC	DG3	Mouse IgG1	Human	Miltenyi Biotec #130-095-198
CD105-PE	43A4E1	Mouse IgG1	Human	Miltenyi Biotec #130-095-198
CD133	polyclonal	Rabbit IgG	Human	Abcam #ab16518
CD206- eFluor450	19.2	Mouse IgG1κ	Human	eBioscience #48-2069-41
CD271-FITC	ME20.4-1.H4	Mouse IgG1	Human	Miltenyi Biotec #130-91-917
CD318	polyclonal	Rabbit IgG	Human	Bioss #5880-R
Dectin-1-PE	15E2	Mouse IgG2a κ	Human	eBioscience #12-9856-42
IL-12/IL23 p40-eFluor450	EBioHP40	Mouse IgG1 κ	Human	eBioscience #48-7235-41
MelanA	1F12	Mouse IgG1	Human	LifeSpan Biosciences #LS-C174654
SSEA4-PE	MC-813-70	Mouse IgG3	Human	eBioscience #12-8843-71
TNFα-PerCP-Cy5.5	MAb11	Mouse IgG1 κ	Human	eBioscience #45-7349-41
Arginase 1-PE	polyclonal	Sheep IgG	Mouse	R&D Systems #IC5868P
CD206-AF647	C068C2	Rat IgG2a κ	Mouse	BioLegend #141711
Dectin-1-FITC	REA154	Rec. human IgG1	Mouse	Miltenyi Biotec #130-102-986
IL12/IL23 p40-PerCp-Cy5.5	C17.8	Rat IgG2a κ	Mouse	eBioscience #45-7123-80
NOS2-PE	CXNFT	Rat IgG2a κ	Mouse	eBioscience #12-5920-80
TNF-α-PerCp-Cy5.5	MP6-XT22	Rat IgG1 κ	Mouse	BioLegend #506322